# H$\alpha$ Imaging of X-ray Sources in Selected Globular Clusters with the SOAR Telescope



**Paweł P i e t r u k o w i c z**

Departamento de Astronomía y Astrofísica, Pontificia Universidad Católica de Chile, Av. Vicuña MacKenna 4860, Casilla 306, Santiago 22, Chile
Nicolaus Copernicus Astronomical Center, ul. Bartycka 18, 00-716 Warszawa, Poland
e-mail: pietruk@astro.puc.cl

ABSTRACT

We present results of a search for objects with H$\alpha$ excess, such as cataclysmic variables (CVs) and chromospherically active binaries (ABs), as counterparts to X-ray sources detected with Chandra satellite observatory in six Galactic globular clusters (GCs): M4, M28, M30, M71, M80, NGC 6752. Binary systems play a critical role in the evolution of GCs, serving as an internal energy source countering the tendency of GC cores to collapse. Theoretical studies predict dozens of CVs in the cores of some GCs (*e.g.*, 130 for M28, 40 for M30). A number of such binaries is also expected outside the core radius. However, few CVs are known so far in GCs. Using subtraction technique applied to images taken with the 4.1-m SOAR telescope we have found 27 objects with H$\alpha$ excess in the field of the observed clusters, of which nine are likely associated with the clusters. Four are candidate CVs, four candidate ABs, one could be either a CV or an AB. One H$\alpha$ object seems to be a background galaxy, while other 17 detected objects are probably foreground or background stars.

*Stars: binaries: close – Stars: activity – Stars: chromospheres – Stars: dwarf novae – novae, cataclysmic variables – Hertzsprung-Russell (HR) and C-M diagrams – globular clusters: individual: M4 (NGC 6121), M28 (NGC 6626), M30 (NGC 7099), M71 (NGC 6838), M80 (NGC 6093), NGC 6752*

## 1 Introduction

Globular clusters are excellent laboratories for the studies of dynamical processes in dense stellar environments. It is well established on theoretical grounds that close binary stars drive the dynamical evolution of GCs (Stodółkiewicz 1986, Hut *et al.* 1992). For example, the presence of the binary stars can delay or halt the evolution of a cluster toward core collapse. Frequent encounters between passing binaries and single stars may produce tightly bound systems forming a variety of exotic objects such as cataclysmic variables (CVs), quiescent low-mass X-ray binaries (qLMXBs), and blue stragglers.

Cataclysmic variables are interacting binaries containing a main-sequence or slightly evolved secondary star losing mass via Roche lobe overflow onto a white dwarf primary. If the strength of the white dwarf's magnetic field is weak ($B < 10^5$ G) then an accretion disk forms. It is believed that the disk thermal instability is the cause of repetitive outbursts observed in some CVs called dwarf novae (DNe). Cataclysmic variables in quiescence typically have absolute magnitudes $6 < M_V < 12$. One of the characteristic observational features of disk CVs in quiescence is the presence of hydrogen emission lines. CVs have X-ray luminosities $L_{\rm X} < 10^{33}$ erg s$^{-1}$. Quiescent CVs lie on or near cluster main sequences, $\gtrsim$2 mag below the turn-off in optical color-magnitude diagrams (CMDs).

A recent, extensive photometric survey by Pietrukowicz *et al.* (2008) has shown that DNe in GCs are very rare indeed. On the other hand, theoretical

studies predict dozens of CVs in GC cores (*e.g.*, Ivanova *et al.* 2006). For example, we expect about 200, 130 and 40 CVs in the cores of 47 Tuc, M28 and M30, respectively. A number of such binaries (mostly primordial) is also expected outside the core radius or even the half-mass radius. As an example, dwarf novae M5-V101 (Oosterhoff 1941) and M22-CV2 (Pietrukowicz *et al.* 2005) are located about two half-mass radii from the cluster centers.

Chromospherically and magnetically active binaries (ABs) have X-ray luminosities similar to those of CVs. There are three types of AB systems: detached binaries comprised of a main-sequence star and a giant or a subgiant (RS CVn systems), detached binaries comprised of two main-sequence stars (BY Dra systems), and contact binaries (W UMa systems). ABs typically can be found on or somewhat above the cluster main sequence or along the subgiant branch in CMDs. Some blue stragglers are observed as contact binaries and can be active. It is believed that, in all these kinds of systems, the magnetic activity is a result of differential rotation and convection in the companion stars controlled by tidal forces and mass transfer between them. Active chromospheres of the stars are dominated by strong H$\alpha$ emission line at a wavelength of 6562.81 Å.

In this paper we present the results of a search for objects with H$\alpha$ excess, mainly CVs and ABs, as counterparts to X-ray sources in six selected globular clusters. Section 2 gives details on the observations and data reductions. Section 3 describes the detected H$\alpha$ objects in each of the clusters, including tentative classification. Finally, Section 4 states our main conclusions.

## 2 Observations and Data Reductions

The observations were carried out on the night of 2008 Aug 7 using the SOAR Optical Imager (SOI) mounted on the 4.1-m Southern Astrophysical Research (SOAR) telescope located on Cerro Pachón, Chile. The imager consists of two $2048 \times 4096$ pixel CCDs spaced 102 pixels apart along their long sides. Each of the CCDs is read by two amplifiers. The total field of view of SOI is $5\farcm24 \times 5\farcm24$. We used $2 \times 2$ binning, which resulted in a resolution of 0.153 arcsec/pixel. To cover the whole $8\farcm8 \times 8\farcm8$ Chandra field of view and to fill the $7\farcs8$ gaps between the individual CCD images, six (or in some cases only four) single exposures were taken in each filter. The following three filters were used: $B$ (central wavelength $\lambda_0 = 4185$ Å, fwhm $\Delta\lambda = 1030$ Å), $R$ ($\lambda_0 = 6437$ Å, $\Delta\lambda = 1525$ Å), and H$\alpha$ ($\lambda_0 = 6563$ Å, $\Delta\lambda = 75$ Å), with exposure times of 150 s, 200 s and 500 s, respectively. We observed six Galactic globular clusters: M4, M28, M30, M71, M80 and NGC 6752. Tables 1 and 2 give basic physical facts on the clusters, such as reddening, distance modulus, and metallicity, while Table 3 presents information on timing, airmasses, and seeing conditions during the observations.

All images were de-biased and flat-fielded using SOI Reduction Scripts*. With the help of the *Difference Image Analysis Package* (DIAPL)†, which is a modified version of DIA written by Woźniak (2000), we subtracted $R$-band images from images taken in the H$\alpha$ filter (or vice versa if an H$\alpha$ image had a lower seeing). We used the ESO Online Digital Sky Survey (DSS) to set equatorial coordinates in each image. This operation was done with an accuracy better than $1\farcs0$. All X-ray regions in H$\alpha - R$ residual images were inspected by eye.

*The scripts were taken from http://khan.pa.msu.edu/www/SOI/

†The package is available at http://users.camk.edu.pl/pych/DIAPL/

For construction of color-magnitude diagrams we extracted profile photometry using the DAOPHOT/ALLSTAR package (Stetson 1987). The H$\alpha$ magnitudes were calibrated by adopting $R-\mathrm{H}\alpha=0$ for the bulk of the stars. For all CMDs the $B$ and $R$ magnitudes were scaled to an exposure time of 1.0 s. Each diagram shows only stars from a single image, read by one amplifier, containing the central part of a cluster, plus overlaid H$\alpha$-excess objects detected in the whole observed field of the cluster.

Table 1: General information on analyzed globular clusters (part 1 of 2).

| NGC | Other name | RA(2000) | Dec(2000) | $E(B-V)$ [mag] | $(m-M)_V$ [mag] |
|---|---|---|---|---|---|
| 6093 | M80 | $16^{\mathrm{h}}17^{\mathrm{m}}02\overset{\mathrm{s}}{.}5$ | $-22^\circ58'30''$ | $0.17\pm0.03^a$ | $15.58\pm0.12^a$ |
| 6121 | M4 | $16^{\mathrm{h}}23^{\mathrm{m}}35\overset{\mathrm{s}}{.}5$ | $-26^\circ31'31''$ | $0.33\pm0.01^b$ | $12.51\pm0.09^c$ |
| 6626 | M28 | $18^{\mathrm{h}}24^{\mathrm{m}}32\overset{\mathrm{s}}{.}9$ | $-24^\circ52'12''$ | $0.42\pm0.02^d$ | $13.4\div13.5^d$ |
| 6752 | | $19^{\mathrm{h}}10^{\mathrm{m}}52\overset{\mathrm{s}}{.}0$ | $-59^\circ59'05''$ | $0.046\pm0.005^e$ | $13.24\pm0.08^e$ |
| 6838 | M71 | $19^{\mathrm{h}}53^{\mathrm{m}}46\overset{\mathrm{s}}{.}1$ | $+18^\circ46'42''$ | $0.28\pm0.06^f$ | $13.71\pm0.11^f$ |
| 7099 | M30 | $21^{\mathrm{h}}40^{\mathrm{m}}22\overset{\mathrm{s}}{.}0$ | $-23^\circ10'45''$ | $0.06\pm0.02^g$ | $14.65\pm0.12^g$ |

The columns give respectively: identification names, equatorial coordinates of the centers, reddening $E(B-V)$, distance modulus $(m-M)_V$. Coordinates were taken from Harris (1996), while other references are given below the table.

References: [a] Brocato *et al.* (1998), [b] Ivans *et al.* (1999), [c] Richer *et al.* (1997), [d] Davidge *et al.* (1996), [e] Gratton *et al.* (2005), [f] Grundahl *et al.* (2002), [g] Sandquist *et al.* (1999)

Table 2: General information on analyzed globular clusters (part 2 of 2).

| NGC | [Fe/H] | $r_\mathrm{c}$ ['] | $r_\mathrm{h}$ ['] | log $\rho_0$ [$\mathrm{L_\odot\ pc^{-3}}$] | $N_\mathrm{CV}$ | Remarks |
|---|---|---|---|---|---|---|
| 6093 | $-1.71\pm0.20^a$ | 0.15 | 0.65 | 4.76 | 169 | |
| 6121 | $-1.17\pm0.31^b$ | 0.83 | 3.65 | 3.82 | 4.8 | |
| 6626 | $-1.37\pm0.03^c$ | 0.24 | 1.56 | 4.73 | 130 | |
| 6752 | $-1.48\pm0.07^d$ | 0.17 | 2.34 | 4.91 | 51 | ccc |
| 6838 | $-0.71\pm0.11^e$ | 0.63 | 1.65 | 3.04 | 39 | |
| 7099 | $-2.01\pm0.09^f$ | 0.06 | 1.15 | 5.04 | 39 | ccc |

The columns give respectively: identification name, metallicity [Fe/H], core radius $r_\mathrm{c}$, half-mass radius $r_\mathrm{h}$, central density $\rho_0$, predicted number of CVs in cores of the clusters. All values but metallicities (see table footnotes) were taken from Harris (1996). The predicted number of CVs in the cores of the clusters was scaled to $N_\mathrm{CV}=200$ for 47 Tucanae according to formula, given by Pooley *et al.* (2003), that the encounter rate $\Gamma\propto\rho_0^{1.5}r_\mathrm{c}^2$.

References: [a] Brocato *et al.* (1998), [b] Drake *et al.* (1994), [c] Davidge *et al.* (1996), [d] Gratton *et al.* (2003), [e] Grundahl *et al.* (2002), [f] Sandquist *et al.* (1999)

Remarks: ccc – core-collapsed cluster

# 3 Detected H$\alpha$ objects

We have detected 27 objects with H$\alpha$ emission around X-ray sources in six observed globular clusters. Table 4 gives coordinates of the objects, identifications of their X-ray counterparts, and tentative classification. Figures 1-2 show finding charts in the $R$ band, and corresponding $\mathrm{H}\alpha-R$ residual images for all

Table 3: Short log of SOAR observations on the night of 2008 Aug 7/8

| NGC | UT [hh:mm] | Airmass | Seeing in $R$ [$''$] |
|---|---|---|---|
| 6093 | 23:12–01:02 | 1.02–1.05 | 0.56–0.79 |
| 6121 | 01:12–03:01 | 1.05–1.31 | 0.63–0.84 |
| 6626 | 03:22–05:03 | 1.06–1.33 | 0.68–1.09 |
| 6838 | 05:16–06:15 | 1.78–2.24 | 0.87–0.98 |
| 6752 | 06:36–07:38 | 1.51–1.79 | 0.80–1.10 |
| 7099 | 07:51–08:54 | 1.23–1.53 | 0.78–0.88 |

objects. Below we describe in detail all H$\alpha$ objects we have found in each of the six observed clusters.

## 3.1 NGC 6093 (M80)

This low-metallicity globular cluster has small core and half-mass radii of only $9''$and $39''$, respectively. NGC 6093 is unusual in having a variety of exotic objects. It has one of the largest and most concentrated population of blue stragglers (over 300) ever observed in a globular cluster (Ferraro *et al.* 1999). NGC 6093 is known to harbor two dwarf novae (DN1 and DN2, Shara *et al.* 2005) and a classical nova (nova 1860 T Sco, Shara and Drissen 1995). The cluster's X-ray population is rich. Using Chandra satellite observatory Heinke *et al.* (2003) detected some 19 sources within the half-mass radius, and an additional 52 sources within $9'$ from the cluster center. Soft X-ray spectra of two bright inside sources indicates that they are probable qLMXBs. Five sources with hard spectra were classified as likely CVs. According to theoretical calculations (see Table 2), we expect about 170 CVs in the core of NGC 6093. The reason for such a large number of binaries in this cluster is its high stellar density, and dynamical state near core-collapse.

We detected two H$\alpha$-emission objects around X-ray sources in the field of NGC 6093. Finding charts are presented in Fig. 1. Both of them lie outside the half-mass radius: $1.6r_{\rm h}$ and $11.5r_{\rm h}$ from the center. The first one, object #2, is faint, but has relatively large H$\alpha$ excess (see Fig. 3). Although it was not possible to measure its brightness in the $B$ band, this object is a good candidate for an AB. Object #1 is bright, but its location in the $R$ *vs.* $B-R$ diagram (Fig.3) and large angular distance from the cluster center rather rule out this star as a member of NGC 6093.

The searches for counterparts to X-ray sources in this cluster confirms that source 161714.6-225520 in Heinke *et al.* (2003) coincides with the position of the bright star HD 146457 ($V=8.46$ mag), which is saturated in our images. We note that the following X-ray sources are located outside the analyzed field of view: J161648.5-225311, J161701.0-225307, J161706.4-225318, J161712.3-225313, J161713.6-225324, and J161721.7-225415.

## 3.2 NGC 6121 (M4)

NGC 6121 is the closest globular cluster (1.73 kpc, Richer *et al.* 1997). The core and half-mass radii of this cluster are $0\farcm83$ and $3\farcm65$, respectively. NGC 6121 has a relatively low collision number $\Gamma$, resulting from a relatively low central density $\rho_0$. Thus the expected number of CVs in the core is not larger than five. Bassa

Table 4: Coordinates, X-ray counterparts, and classification of detected objects with H$\alpha$ excess. Objects not classified are very likely foreground or background stars.

| H$\alpha$ object | RA(2000.0) | Dec(2000.0) | Distance from the center | ID number of X-ray source | Class. |
|---|---|---|---|---|---|
| NGC6093-1 | $16^{\rm h}16^{\rm m}46^{\rm s}.87$ | $-22°55'09''.6$ | $7'.47$ | J161646.9-225509[a] | |
| NGC6093-2 | $16^{\rm h}17^{\rm m}06^{\rm s}.14$ | $-22°58'35''.6$ | $1'.06$ | J161706.2-225835[a] | AB? |
| NGC6121-1 | $16^{\rm h}23^{\rm m}34^{\rm s}.44$ | $-26°32'00''.2$ | $0'.56$ | CX13[b] | AB |
| NGC6121-2 | $16^{\rm h}23^{\rm m}36^{\rm s}.94$ | $-26°31'44''.5$ | $0'.42$ | CX15[b] | |
| NGC6121-3 | $16^{\rm h}23^{\rm m}40^{\rm s}.25$ | $-26°29'25''.6$ | $2'.40$ | CX23[b] | CV |
| NGC6121-4 | $16^{\rm h}23^{\rm m}42^{\rm s}.68$ | $-26°31'45''.1$ | $1'.82$ | CX24[b] | CV |
| NGC6626-1 | $18^{\rm h}24^{\rm m}20^{\rm s}.62$ | $-24°51'26''.9$ | $2'.23$ | #2[c] | AB |
| NGC6626-2 | $18^{\rm h}24^{\rm m}22^{\rm s}.85$ | $-24°52'45''.7$ | $2'.49$ | #5[c] | |
| NGC6626-3 | $18^{\rm h}24^{\rm m}24^{\rm s}.24$ | $-24°51'03''.4$ | $2'.46$ | #6[c] | |
| NGC6626-4 | $18^{\rm h}24^{\rm m}24^{\rm s}.63$ | $-24°53'01''.1$ | $2'.08$ | #7[c] | AB/CV |
| NGC6626-5 | $18^{\rm h}24^{\rm m}25^{\rm s}.21$ | $-24°54'06''.1$ | $2'.70$ | #8[c] | AB? |
| NGC6626-6 | $18^{\rm h}24^{\rm m}32^{\rm s}.41$ | $-24°53'52''.2$ | $2'.37$ | #20[c] | AB? |
| NGC6626-7 | $18^{\rm h}24^{\rm m}33^{\rm s}.70$ | $-24°52'13''.6$ | $1'.67$ | #32[c] | AB |
| NGC6626-8 | $18^{\rm h}24^{\rm m}36^{\rm s}.61$ | $-24°50'19''.6$ | $2'.59$ | #38[c] | |
| NGC6626-9 | $18^{\rm h}24^{\rm m}37^{\rm s}.34$ | $-24°51'55''.2$ | $1'.14$ | #39[c] | |
| NGC6626-10 | $18^{\rm h}24^{\rm m}38^{\rm s}.93$ | $-24°51'45''.7$ | $3'.17$ | #40[c] | |
| NGC6626-11 | $18^{\rm h}24^{\rm m}39^{\rm s}.50$ | $-24°50'29''.7$ | $0'.46$ | #43[c] | |
| NGC6626-12 | $18^{\rm h}24^{\rm m}40^{\rm s}.26$ | $-24°51'34''.5$ | $1'.96$ | #44[c] | |
| NGC6626-13 | $18^{\rm h}24^{\rm m}42^{\rm s}.63$ | $-24°52'47''.3$ | $0'.20$ | #46[c] | |
| NGC6752-1 | $19^{\rm h}10^{\rm m}56^{\rm s}.26$ | $-59°59'37''.8$ | $1'.21$ | CX2[d] | CV |
| NGC6838-1 | $19^{\rm h}53^{\rm m}42^{\rm s}.65$ | $+18°45'47''.9$ | $1'.26$ | s02[e] | |
| NGC6838-2 | $19^{\rm h}53^{\rm m}43^{\rm s}.84$ | $+18°44'27''.0$ | $2'.32$ | s48[e] | |
| NGC6838-3 | $19^{\rm h}53^{\rm m}44^{\rm s}.56$ | $+18°48'19''.9$ | $1'.68$ | s49[e] | |
| NGC6838-4 | $19^{\rm h}53^{\rm m}52^{\rm s}.75$ | $+18°47'52''.2$ | $2'.02$ | s57[e] | CV? |
| NGC6838-5 | $19^{\rm h}53^{\rm m}52^{\rm s}.80$ | $+18°46'35''.0$ | $1'.68$ | s28[e] | gal |
| NGC7099-1 | $21^{\rm h}40^{\rm m}16^{\rm s}.30$ | $-23°08'20''.1$ | $2'.81$ | #33[f] | CV |
| NGC7099-2 | $21^{\rm h}40^{\rm m}21^{\rm s}.44$ | $-23°06'50''.6$ | $3'.90$ | #46[f] | AB |

References: [a] Heinke *et al.* (2003), [b] Bassa *et al.* (2004), [c] Becker *et al.* (2003), [d] Pooley *et al.* (2002), [e] Elsner *et al.* (2008), [f] Lugger *et al.* (2007)

*et al.* (2004) report on detection of 31 X-ray sources with luminosities down to $L_{\rm X} \approx 10^{29}$ erg s$^{-1}$. According to the authors three sources (CX1, CX2, and CX4) are probable CVs, because they have a relatively high X-ray-to-optical flux ratio. One source (CX12) was classified as a millisecond pulsar, and 12 sources as chromospherically active binaries.

The SOAR data allowed us to detect four stars with H$\alpha$ emission around X-ray sources (see charts in Fig. 1). All of them are located inside the half-mass radius, while two stars, #1 and #2, even inside the core radius. The two stars in the core are brighter respectively by about 2 mag and 1 mag in $R$ than stars #3 and #4. Figure 4 shows two color-magnitude diagrams with positions of the four detected H$\alpha$ objects. Objects #1 and #2 coincide respectively with W UMa-type variables V49 and V48 from Kaluzny *et al.* (1997). The star #2 is a candidate blue straggler and could be chromospherically active. The system #1 is a likely field star, since it is observed about 0.2 mag to the red of the main sequence and 0.5 mag below turn-off in the $R$ *vs.* $B-R$ diagram. The CMD

location of star #3 supports the hypothesis that this is a CV in quiescence in NGC 6121. The position of star #4 is consistent with both the AB and CV interpretations, although the first one seems to be more plausible.

### 3.3 NGC 6626 (M28)

NGC 6626 is located only 9.°6 from the Galactic center at ($l$,$b$)=(7.°80,−5.°58), the most central of all clusters studied here. It has a moderate reddening of $E(B-V)=0.42$ and an average globular cluster metallicity of [Fe/H]$=-1.37$ (Davidge *et al.* 1996). Chandra observations of NGC 6626 allowed us to discover 46 X-ray sources, of which 12 lie within its 0.′24 core radius (Becker *et al.* 2003). Spectral analysis indicates that six of these sources are neutron stars, including the pulsar PSR B1821–24.

Our SOAR images have revealed 13 objects with H$\alpha$ excess in the positions of X-ray sources in the field of this cluster. Charts for these objects can be found in Figs. 1 and 2, while color-magnitude diagrams are presented in Fig. 5. Only three of the newly discovered H$\alpha$ objects, namely #1, #4, and #7, are located on the cluster main-sequence or subgiant branch in the $R$ *vs.* $B-R$ diagram, though it is not clear if source #4 is a star. Objects #1 and #7 are good candidates for RS CVn systems in NGC 6626. The other objects with H$\alpha$ excess are likely foreground or background stars, including star #13 which is located only $0.83r_{\rm c}$ from the cluster center.

### 3.4 NGC 6752

This core-collapsed globular cluster was observed with the Chandra X-ray observatory on 2000 May 15. Pooley *et al.* (2002) report on detection of 19 point sources within the cluster half-mass radius. Based on X-ray and optical properties, they found 10 likely CVs, one to three likely chromospherically active systems, and two possible extragalactic objects. They detected another 21 sources outside the half-mass radius, but there is no information available on these sources. Using archival H$\alpha$ images of the central region of NGC 6752, taken with the WFPC2 camera on board HST, Pooley *et al.* (2002) show that the optical counterparts to X-ray sources CX1, CX2, CX4, and CX7 have clear H$\alpha$ excess. All four sources were classified as CVs due to their characteristic X-ray spectra (3 keV thermal bremsstrahlung).

In the SOAR data, only source CX2, located 1.′21 from the cluster center, has a noticeable H$\alpha$ emission. The other three sources mentioned above are located at least three times closer to the center, with CX4 and CX7 inside the core radius of 0.′17. For NGC 6752 we present only charts centered on the optical counterpart of CX2 (see upper middle panel in Fig. 2). Unfortunately, the star is not measurable in any of the SOAR images.

### 3.5 NGC 6838 (M71)

This globular cluster is the most metal-rich ([Fe/H]$=-0.71$, Grundahl *et al.* 2002) and has the closest location to the Galactic plane ($b$=−4.°56) among the six clusters observed with SOAR. The X-ray population of NGC 6838 was recently studied by Elsner *et al.* (2008) with the Chandra X-ray observatory. They found five sources located within the 0.′63 cluster core radius, another 24 sources within the 1.′65 half-mass radius, 34 sources with $r_{\rm h}<r<2r_{\rm h}$, and 73 sources outside $2r_{\rm h}$. One of the five sources in the core is associated with the pulsar M71A. For

many X-ray sources located outside the core the authors give possible optical and infrared counterparts in the 2MASS, USNO B1.0 and TYCHO-2 catalogs. None of the sources is suspected to be a cataclysmic variable.

Searches for H$\alpha$-emission objects in NGC 6838 with the SOAR telescope have brought about five identifications. Finding charts for these objects are included in Fig. 2, while $R$ *vs.* H$\alpha - R$ and $R$ *vs.* $B-R$ CMDs are presented in Fig. 6. All detections but object #5 (associated with the X-ray source s28) are of stellar nature. Star #2 lies very close to the edge of the CCD, and for this reason it is absent in both color-magnitude diagrams. Stars #1 and #3 are located too far from the cluster main sequence in the $R$ *vs.* $B-R$ diagram that their membership status is out of question. The only object which might be a CV is object #4. Unfortunately it is surrounded by bright stars, and no information on $B-R$ color was obtained. Source #5, due to its elongated shape, could be a starburst galaxy.

It is very likely that the X-ray source s52 is the bright ($V = 10.76$ mag) foreground star HD 350790. We also note that some of the X-ray sources could not be checked, since they lie either inside the gaps between the CCDs of the SOI camera (s34–s37) or outside the whole investigated field of NGC 6838 (s61–s63, ss01–ss15, ss24, ss31, ss37–ss59).

### 3.6 NGC 7099 (M30)

NGC 7099 has a low reddening of $E(B-V)$=0.06±0.02 and a distance modulus of $(m-M)_V$=14.65±0.12 (Sandquist *et al.* 1999). It is the second core-collapsed cluster in our sample. According to Harris (1996), the central part of NGC 7099 represents one of the highest density environments in the Galaxy. Thus, a large population of compact binaries is expected in this cluster. X-ray observations with Chandra (Lugger *et al.* 2007) revealed 50 sources within $4\farcm5$ from the center, with luminosities down to $L_{\rm X} = 4 \times 10^{30}$ erg s$^{-1}$ at the distance of the cluster. The brightest source ($L_{\rm X} = 6 \times 10^{32}$ erg s$^{-1}$) within the $1\farcm15$ half-mass radius, source #2 (also identified as A1), is believed to be a qLMXB. Its blackbody-like soft X-ray spectrum supports this hypothesis. Sources #1 (A2), #3 (A3), #4 (B), and #5 (C) have X-ray properties consistent with being CVs. For sources #7 and #10, Lugger *et al.* (2007) find possible AB counterparts in HST images.

The tiny and dense center of NGC 7099 is very difficult to study using ground-based telescopes. The H$\alpha$ imaging with SOAR allowed us to detect two sources: #1 at a distance of $2.4r_{\rm h}$, and #2 at $3.4r_{\rm h}$. The bottom of Fig. 2 includes charts for these two stellar sources. Their location on the $R$ *vs.* $B-R$ diagram (Fig. 7) favors the hypothesis that both objects belong to the cluster, in spite of their relatively large distance from the center. The fainter source #1, which lies slightly to the blue side of the main sequence ∼2 mag below of the turn-off, is a likely CV. The CMD location of star #2 is consistent with an AB interpretation. Here, we also confirm that a bright foreground star at $\alpha_{2000} = 21^{\rm h}40^{\rm m}33\fs40$, $\delta_{2000} = -23°12'36\farcs2$, which is saturated in the SOAR images, is a counterpart to X-ray source #39. The positions of four X-ray sources, #37, #41, #43, and #50, coincide with the positions of four galaxies in our images.

## 4 Discussion and Summary

We have presented the results of a search for objects with H$\alpha$ excess in the field of six globular clusters: M4, M28, M30, M71, M80, and NGC 6752. In total we

have found 27 objects, of which nine seem to be associated with these clusters. For four objects, due to lack of information on the $B-R$ color, their status membership remains unclear. For one source its elongated image indicates an extragalactic nature. The rest of the detected H$\alpha$ objects are likely foreground or background stars.

The SOAR observations show how difficult it is to peer inside dense centers of Galactic globular clusters using a medium-class, ground-based telescope, even in good seeing conditions. Merely three detected objects are located inside the cores of the investigated clusters, and five more within the half-mass radii (see Fig. 8). Source NGC6752-1 is the only object in the sample known to be a CV. Unfortunately, it lies in a very crowded central region of this core-collapsed globular cluster, and no brightness information could be obtained. For nine objects likely associated with the clusters a tentative classification is given based on their location on a $R$ *vs.* $B-R$ diagram. Four stars have been proposed to be chromospherically active, four are possible CVs, and one object is either an AB or a CV. Two of the four CVs, namely objects NGC6121-3 and NGC6121-4, are located within the half-mass radius of M4, but none of them in the core.

The largest number of H$\alpha$-emission objects (13) has been found in the field of the globular cluster NGC 6626 (M28). This cluster is projected in front of the bulge, and it is not a surprise that at least eight of these objects are foreground/background stars.

We stress that the SOAR observations were performed on one night and that there are only single exposures for most of the stars. Some of the detected H$\alpha$ objects are variable, and the subtraction technique applied here can mimic the H$\alpha$ excess. For example, it is not clear if the H$\alpha$ emission from stars NGC6121-1 and NGC6121-2, reported by Kaluzny *et al.* (1997) as eclipsing/ellipsoidal binaries, is real. A long-term monitoring would solve this problem.

The observed clusters have very different metallicities, reddenings, and dynamical properties. Unfortunately, the small number of detected objects is insufficient to show any tendency, especially since for none of them membership status has been confirmed. For all clusters but NGC 6121 the total number of known CVs in their centers seems to be far too small compared to theoretical predictions. However, one has to take into account that H$\alpha$ emission from many faint ABs and CVs, especially located in the crowded central parts of the clusters, can be very weak or even undetectable. It is very likely that new faint compact binaries such as CVs will be discovered in the near future thanks to the newly refurbished Hubble Space Telescope.

**Acknowledgments.** The author would like to thank Márcio Catelan for important discussions and remarks on the draft version of this paper. The author is supported by the Chilean FONDAP Center for Astrophysics No. 15010003, the Polish Ministry of Science and Higher Education through the grant N N203 301335, and the Foundation for Polish Science through program MISTRZ.

# REFERENCES

Bassa, C., Pooley, D., Homer, L., Verbunt, F., Gaensler, B.M., Lewin W.H.G., Anderson, S.F., Margon, B., Kaspi, V.M., van der Klis M. 2004, *Astrophys. J.*, **609**, 755.

Becker, W., Swartz, D.A., Pavlov, G.G., Elsner, R.F., Grindlay, J., Mignani, R., Tennant, A.F., Backer, D., Pulone, L., Testa, V., Weisskopf, M.C. 2003, *Astrophys. J.*, **594**, 798.

Brocato, E., Castellani, V., Scotti, G.A., Saviane, I., Piotto, G., Ferraro, F.R. 1998, *Astron. Astrophys.*, **335**, 929.
Davidge, T.J., Cote, P., and Harris, W.E. 1996, *Astrophys. J.*, **468**, 641.
Drake, J.J., Smith, V.V., and Suntzeff, N.B. 1994, *Astrophys. J.*, **430**, 610.
Elsner, R.F., Heinke, C.O., Haldan, N.C., Lugger, P.M., Maxwell, J.E., Stairs, I.H., Ransom, S.M., Hessels, W.T.J, Becker, W., Huang, R.H.H., Edmonds, P.D., Grindlay, J.E., Bogdanov, S., Ghosh, K., Weisskopf, M.C. 2008, *Astrophys. J.*, **687**, 1019.
Ferraro, F.R., Paltrinieri, B., Rood, R.T., and Dorman, B. 1999, *Astrophys. J.*, **522**, 983.
Gratton, R.G., Bragaglia, A., Carretta, E., Clementini, G., Desidera, S., Grundahl, F., Lucatello, S. 2003, *Astron. Astrophys.*, **408**, 529.
Gratton, R.G., Bragaglia, A., Carretta, E., de Angeli, F., Lucatello, S., Piotto, G., Recio Blanco, A. 2005, *Astron. Astrophys.*, **440**, 901.
Grundahl, F., Stetson, P.B., and Andersen, M.I. 2002, *Astron. Astrophys.*, **395**, 481.
Harris, W.E. 1996, *Astron. J.*, **112**, 1487.
Heinke, C.O., Grindlay, J.E., Edmonds, P.D., Lloyd, D.A., Murray, S.S., Cohn, H.N., Lugger, P.M. 2003, *Astrophys. J.*, **598**, 516.
Hut, P. *et al.* 1992, *P.A.S.P.*, **104**, 981.
Ivans, I.I., Sneden, C., Kraft, R.P., Suntzeff, N.B., Smith, V.V., Langer, G.E., Fulbright, J.P. 1999, *Astron. J.*, **118**, 1273.
Ivanova N., Heinke C.O., Rasio F.A., Taam R.E., Belczynski K., Fregeau J. 2006, *MNRAS*, **372**, 1043.
Kaluzny, J., Thompson, I.B., and Krzeminski, W. 1997, *Astron. J.*, **113**, 2219.
Lugger, P.M., Cohn, H.N., Heinke, C.O., Grindlay, J.E., Edmonds, P.D. 2007, *Astrophys. J.*, **657**, 286.
Oosterhoff P.T. 1941, *Ann. Sterrewacht Leiden*, **17**, 4.
Pietrukowicz, P., Kaluzny, J., Schwarzenberg-Czerny, A., Thompson, I.B., Pych, W., Krzemiński, Mazur, B 2008, *MNRAS*, **388**, 1111.
Pietrukowicz, P., Kaluzny, J., Thompson, I.B., Jaroszynski, M., Schwarzenberg-Czerny, A., Krzeminski, W., Pych, W. 2005, *Acta Astron.*, **55**, 261.
Pooley, D., Lewin, W.H.G., Homer, L., Verbunt, F., Anderson, S.F., Gaensler, B.M., Margon, B., Miller, J.M., Fox, D.W., Kaspi, V.M., van der Klis, M. 2002, *Astrophys. J.*, **569**, 405.
Pooley, D. *et al.* 2003, *Astrophys. J.*, **591**, L131.
Richer, H.B. et al. 1997, *Astrophys. J.*, **484**, 741.
Sandquist, E.L., Bolte, M., Langer, G.E., Hesser, J. E., de Oliveira, C.M. 1999, *Astrophys. J.*, **518**, 262.
Shara, M.M., and Drissen, L. 1995, *Astrophys. J.*, **448**, 203.
Shara, M.M., Hinkley, S., and Zurek, D.R. 2005, *Astrophys. J.*, **634**, 1272.
Stetson, P.B. 1987, *P.A.S.P.*, **99**, 191.
Stodółkiewicz, J.S. 1986, *Acta Astron.*, **36**, 19.
Woźniak, P.R. 2000, *Acta Astron.*, **50**, 421.

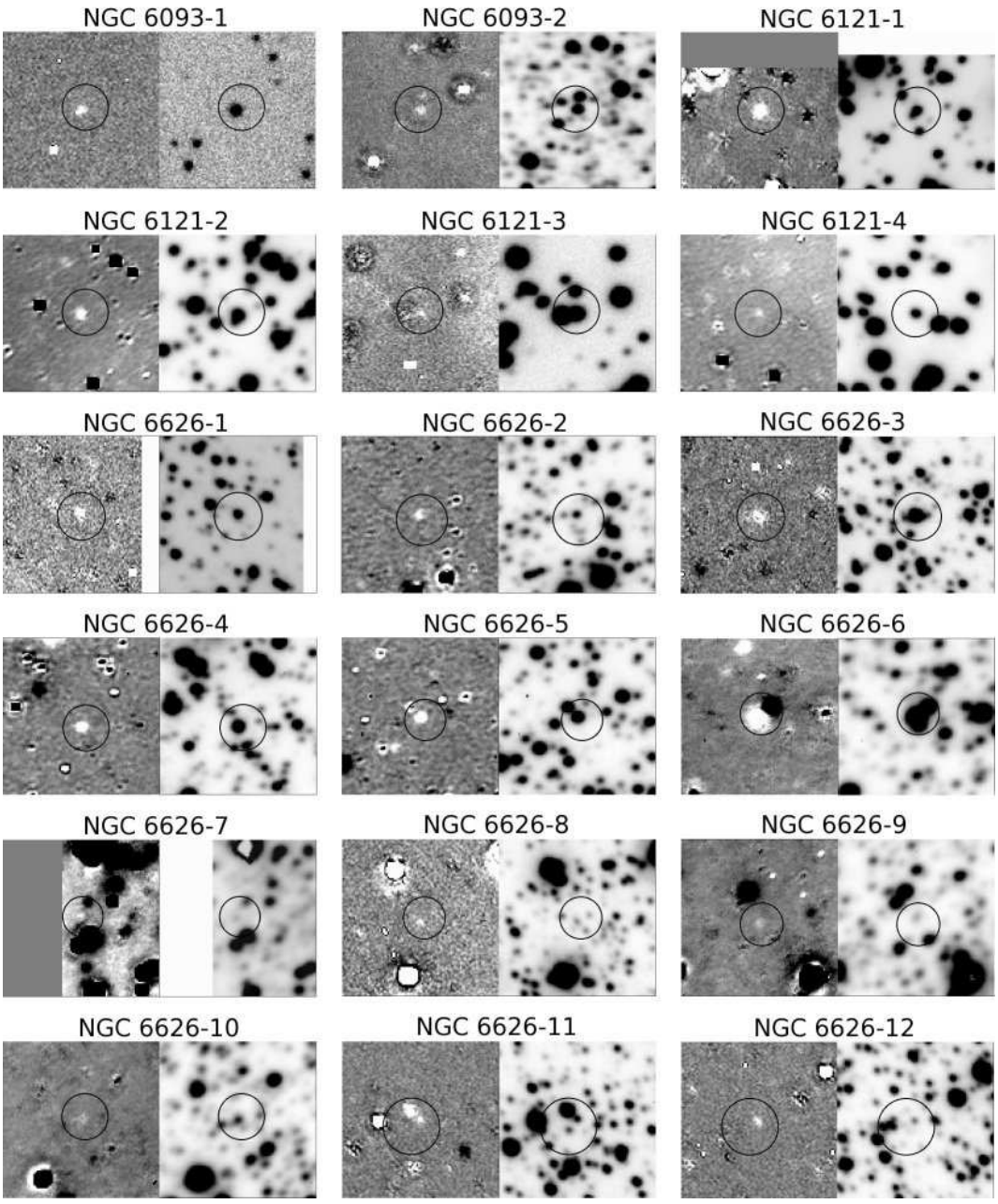


Fig. 1. Charts for detected objects with H$\alpha$ excess (part 1 of 2). The right-hand side panels show $R$-band images, while the left-hand side panels show corresponding H$\alpha - R$ residual images. The 99% confidence uncertainties on X-ray positions are overlaid on the charts. Each chart is $15''$ on a side and centered on an H$\alpha$ source. North is always up and East to the left.

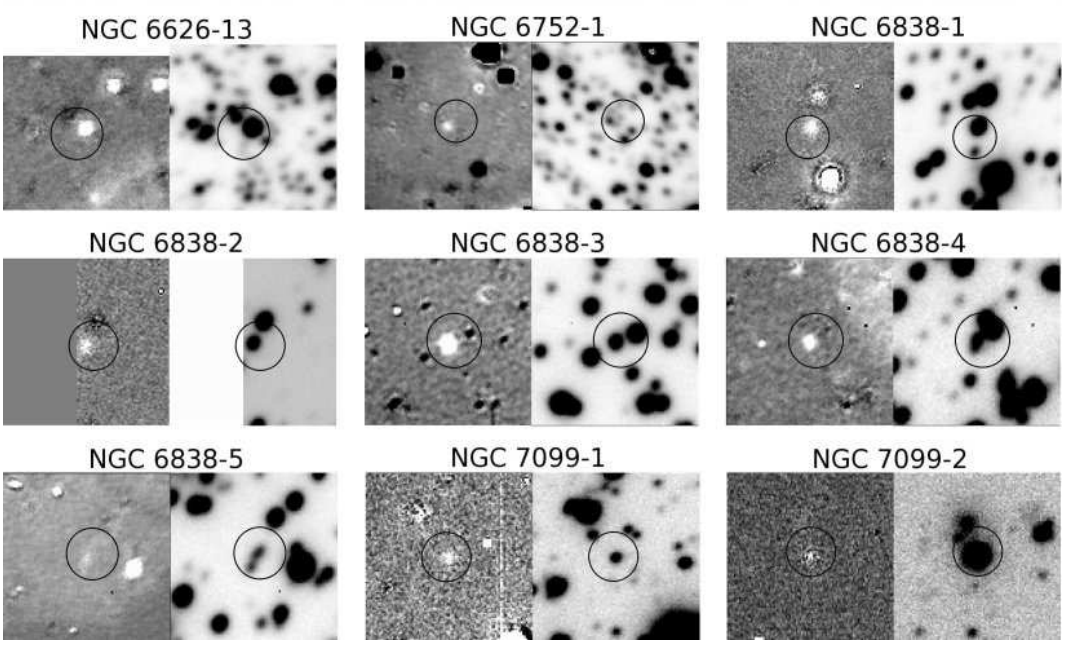


Fig. 2. Charts for detected objects with H$\alpha$ excess (part 2 of 2). The right-hand side panels show $R$-band images, while the left-hand side panels show corresponding H$\alpha - R$ residual images. The 99% confidence uncertainties on X-ray positions are overlaid on the charts. Each chart is $15''$ on a side and centered on an H$\alpha$ source. North is always up and East to the left.

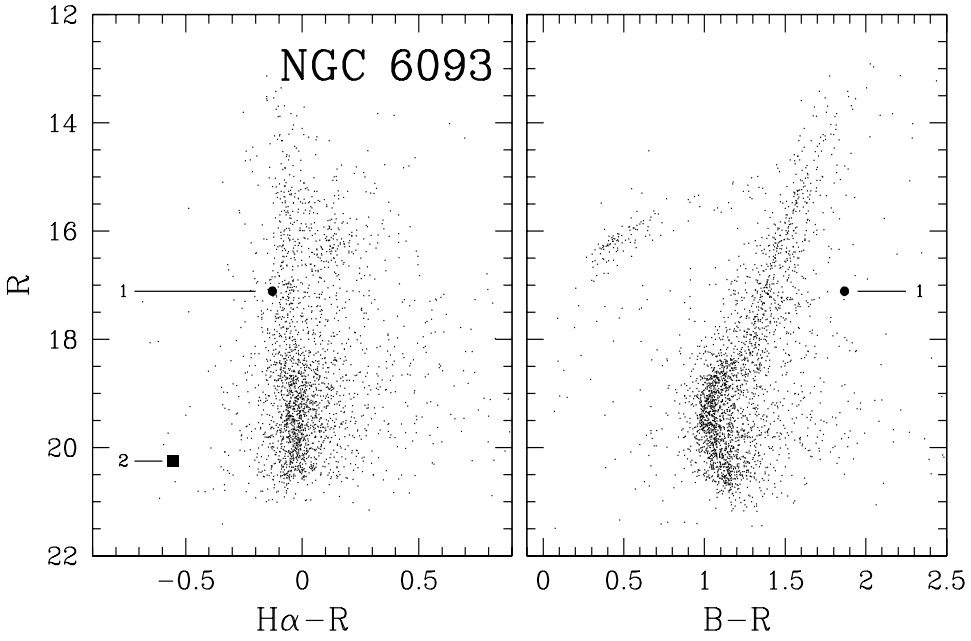


Fig. 3. Color-magnitude diagrams for NGC 6093 (M80). Object #2 could be a chromospherically active binary, though there is no information on its $B - R$ color.

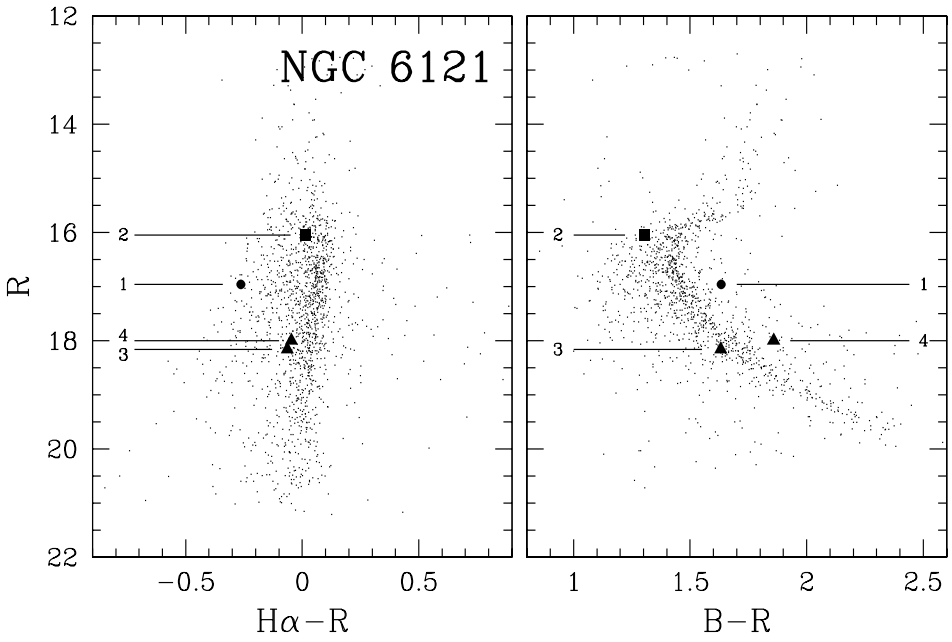


Fig. 4. Color-magnitude diagrams with four Hα objects detected in NGC 6121 (M4). Object #2, marked with a square, is an AB candidate. Triangles denote the location of two possible CVs.

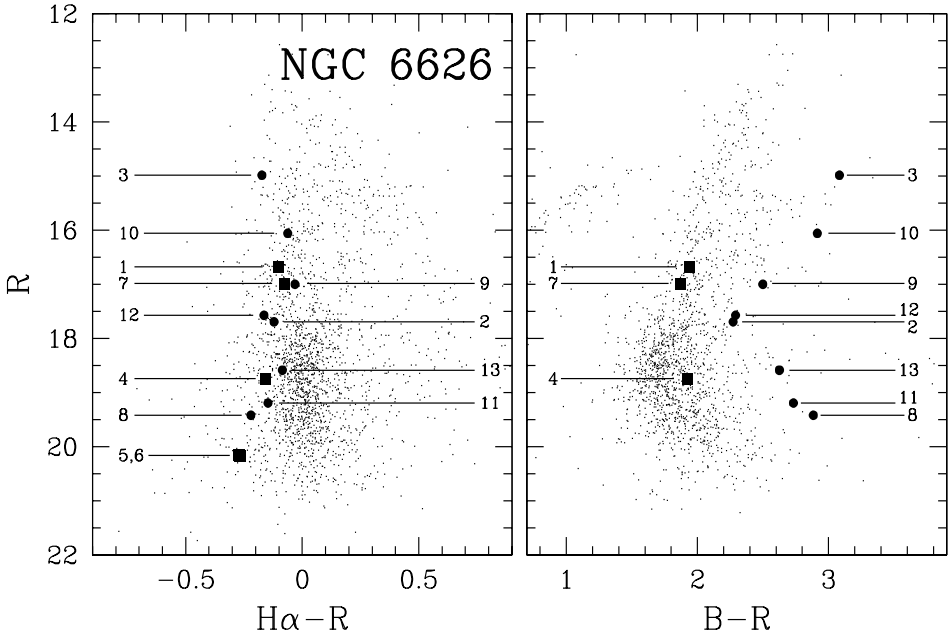


Fig. 5. Color-magnitude diagrams for NGC 6626 (M28). Objects marked with squares are AB candidates.

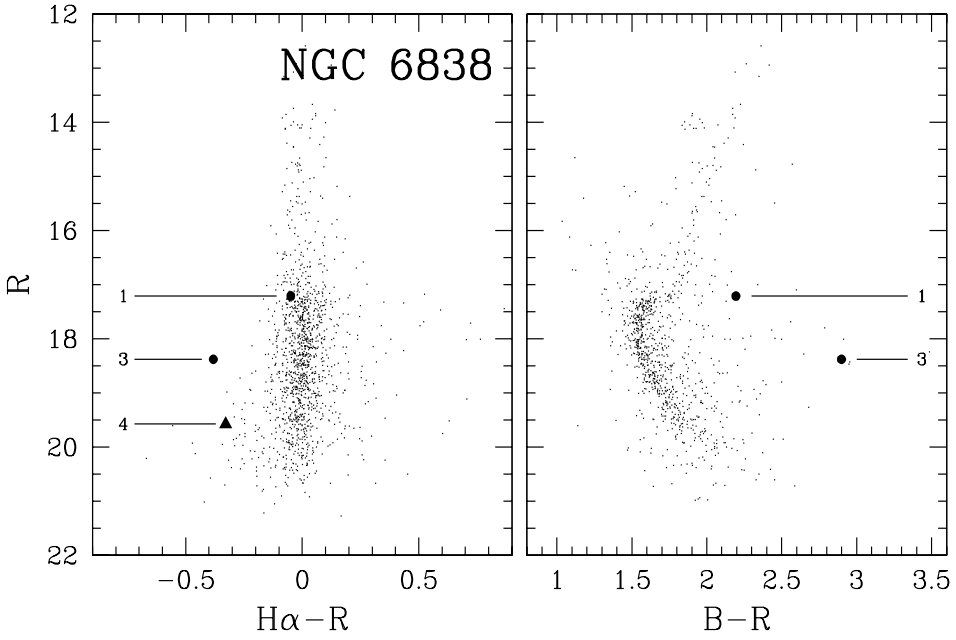


Fig. 6. Color-magnitude diagrams for NGC 6838 (M71). The star marked with a triangle could be a CV, but unfortunately there is no $B-R$ color information for it.

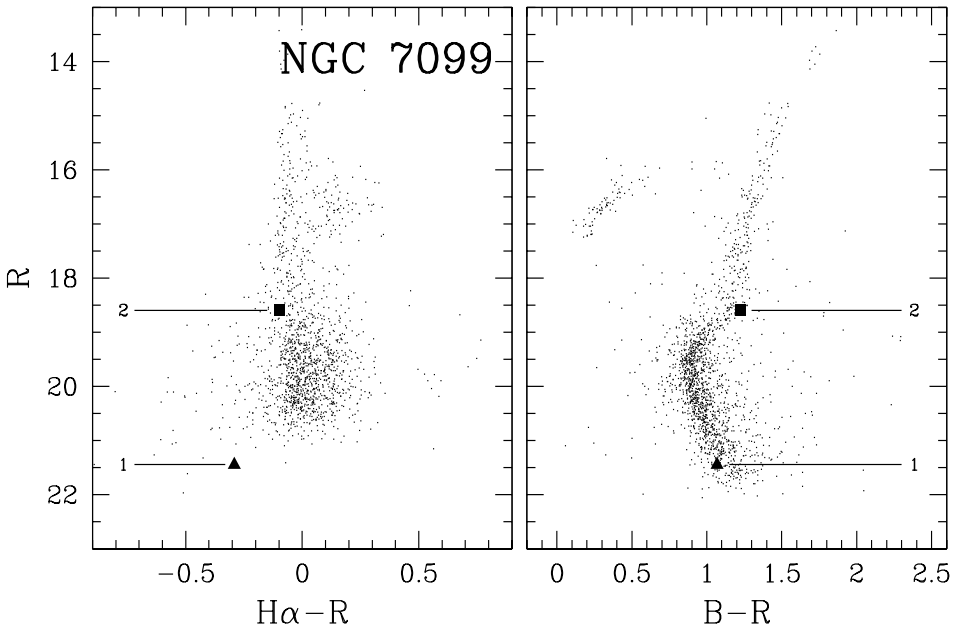


Fig. 7. Optical color-magnitude diagrams for NGC 7099 (M30) with two detected H$\alpha$ objects. Object #1 is a candidate cataclysmic variable, whereas object #2 is a candidate for a chromospherically active binary.

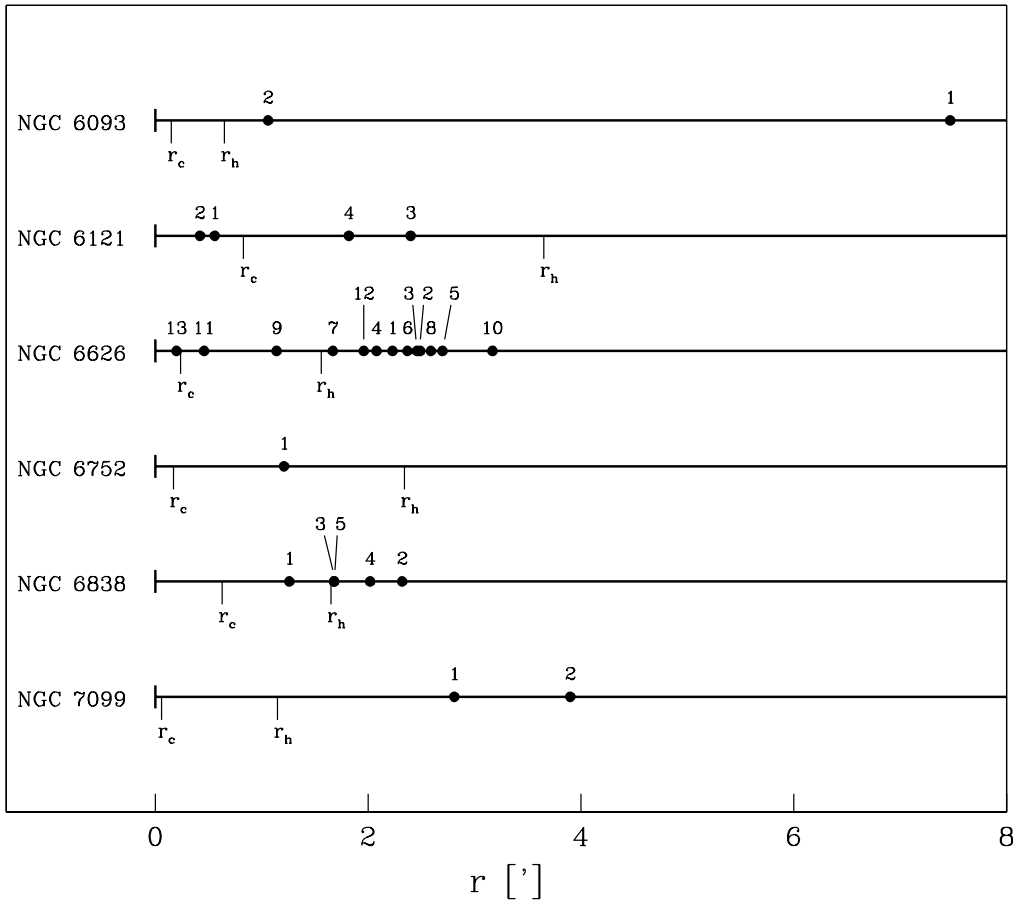


Fig. 8. Distances from the cluster centers of the detected H$\alpha$ objects. Core and half-mass radii are marked for each of the clusters.